



Adsorption of Cr (VI) by chitosan with different deacetylation degrees

Tito Roberto Santana Cadaval Jr., Alisson Schons Camara, Guilherme Luiz Dotto, Luiz Antonio de Almeida Pinto*

Unit Operation Laboratory, School of Chemistry and Food, Federal University of Rio Grande—FURG, Rio Grande, RS, Brazil

Tel. +55 53 3233 8648; Fax: +55 53 3233 8745; email: dqmpinto@furg.br

Received 7 December 2012; Accepted 16 February 2013

ABSTRACT

Chitosan with different deacetylation degrees (DD) was used to remove Cr (VI) from aqueous solution by adsorption. Chitosan was obtained from shrimp wastes and characterized. The adsorption study was carried out by response surface methodology, equilibrium isotherms, thermodynamics, kinetic, and interactions. The results showed that the DD increase caused an increase in chitosan amino groups and changes in crystallinity were observed. The more appropriate conditions for Cr (VI) adsorption by chitosan were DD of 95% and pH 3. The Sips model was the more adequate to fit the experimental equilibrium data ($R^2 > 0.99$ and ARE $< 2.5\%$), and the maximum adsorption capacity was of 97.4 mg g^{-1} , obtained at 298 K. Negative values of ΔH^0 , ΔS^0 , and ΔG^0 showed that the adsorption was exothermic, spontaneous, and favorable. The pseudo-second-order model presented adequate fit with the experimental kinetic data ($R^2 > 0.99$ and ARE < 2.00). It was verified interactions between Cr (VI) and chitosan-protonated amino groups.

Keywords: Adsorption; Chitosan; Deacetylation degree; Isotherms; Kinetic

1. Introduction

Heavy metals occur in natural waters due to discharge of industrial effluents such as, mining, electroplating, iron industries, dry cleaners, oil, and others [1]. The leather tanning industry, for example, generates a great amount of solid and liquid wastes. In this activity, Chromium VI (Cr (VI)) is a highly undesirable type of pollutant. The removal of Cr (VI) is environmentally important due its high toxicity. It is known that effluents containing Cr (VI) are very difficult to treat, since it is highly soluble. Another

difficulty is the treatment of effluents containing Cr (VI) at low concentrations [2]. The conventional methods for water purification, including filtration, chemical precipitation, ion exchange, electrodeposition and membrane systems are unfavorable economically and/or technically complex [3]. Therefore, adsorption is an alternative to remove chromium from aqueous solutions [1,2,4].

In relation to the traditional methods, adsorption provides significant advantages such as easy operation and application, high efficiency, and cost-effectiveness. In addition, environmentally and economically feasible, especially when low cost adsorbents are employed

*Corresponding author.

[3–6]. Commercially, activated carbon is the most common adsorbent to remove heavy metals; however, several alternative adsorbents have been studied, aiming to increase the adsorption capacity and reduce the operating cost, for example: organo-bentonite [7], magnetite [8], phytomass [9], olive stone [10], spider silk [11], rose waster [12], and cow dung powder [13].

Chitosan is a good scavenger for metal ions due its versatility, high efficiency, high selectivity, fast kinetic, availability, and cost-effectiveness [5,14]. It is a biodegradable, hydrophilic and nontoxic aminopolysaccharide, which is obtained from chitin alkaline deacetylation. Chemically is constituted by monomers of D-glucosamine and N-acetylglucosamine [15] and can be obtained from renewable natural sources. Under acid conditions, it is a cationic polysaccharide, being a potential adsorbent [14]. In this context, many studies demonstrated the applicability of chitosan to removal metals, such as copper [16], lead, nickel [17], arsenic [18], zinc, mercury [19], platinum, palladium [6], and chromium [20]. However, these studies used chitosan in the commercial form or modified by many chemical means. An alternative to improve the chitosan performance as adsorbent is obtain this biopolymer with variable deacetylation degree (DD) by changes in its production process [21].

In this work, chitosan with different DD was used to remove Cr (VI) from aqueous solutions. Chitosan was obtained from shrimp wastes and characterized. Cr (VI) adsorption as a function of pH and DD by response surface methodology was optimized. The equilibrium, thermodynamic, and kinetic studies were performed, and also interactions between chitosan and Cr (VI) were elucidated.

2. Materials and methods

2.1. Chitosan production and characterization

Chitosan was obtained from shrimp wastes (*Penaeus brasiliensis*) according to the procedure developed by Weska et al. [22]. The deacetylation reaction was carried out at 40, 90, and 240 min to obtain 75 ± 1 , 85 ± 1 and $95 \pm 1\%$ of DD, respectively [23]. Chitosan was purified [22] and dried in spouted bed [24]. All chitosan samples were sieved until the discrete particle size of $72 \pm 3 \mu\text{m}$.

Chitosan was characterized in relation to DD, viscosity average molecular weight, Fourier transform infrared (FT-IR) and X-ray diffraction (XRD) analysis. The DD was determined by potentiometric linear titration [25]. The chitosan molecular weight was measured by viscosimetric method using Mark-Houwink-Sakurada equation ($K = 1.8 \times 10^{-3} \text{ mL g}^{-1}$

and $\alpha = 0.93$) [23]. The functional groups were identified by FT-IR (Prestige, 21210045, Japan) using diffuse reflectance in KBr pellets [26]. The crystallinity was verified by X-ray diffractometer (Bruker, D2 phaser, Germany). The angle diffraction ranged from 5° to 75° [27].

2.2. Adsorption experiments

The stock Cr (VI) solutions (1.0 g L^{-1}) were prepared from potassium dichromate ($\text{K}_2\text{Cr}_2\text{O}_7$) at different pH values (3, 4, and 5). The pH was adjusted using buffer disodium phosphate/citric acid solution 0.1 mol L^{-1} , and it was measured before and after the adsorption (pHmeter Mars, model MB10, Brazil). The experimental adsorption tests were performed as follows: Firstly, 200 mg of chitosan (dry basis) with different DD (75 ± 1 , 85 ± 1 and 95 ± 1) was added in 100 mL of Cr (VI) solutions (100 mg L^{-1}). After, the solutions were stirred (50 rpm) during 1 h at $298 \pm 1 \text{ K}$ (thermostated shaker Fanem, model 315 SE, Brazil).

In the more adequate condition (obtained by Response Surface Methodology, RSM), experimental runs of isotherms were carried out with Cr (VI) initial concentration ranging from 50 to 400 mg L^{-1} and the temperature from 298 to 328 K, being the solutions stirred until the equilibrium. Kinetic tests were carried out under different stirring rates (50–350 rpm), being aliquots withdrawn at pre-determined times. The Cr (VI) concentration was determined by spectrophotometry (spectrophotometer Quimis, model Q108, Brazil) at 540 nm using 1,5-diphenyl carbazide as the complexing agent [20]. All experiments were carried out in replicate ($n=3$) and blanks were performed. The adsorption capacity (q), equilibrium adsorption capacity (q_e), and adsorption capacity at time t (q_t) were determined by Eqs. (1–3):

$$q = \frac{V(C_0 - C_f)}{m} \quad (1)$$

$$q_e = \frac{V(C_0 - C_e)}{m} \quad (2)$$

$$q_t = \frac{V(C_0 - C_t)}{m} \quad (3)$$

where C_0 is the initial Cr (VI) concentration in liquid phase (mg L^{-1}), C_f is the final Cr (VI) concentration in liquid phase (mg L^{-1}), C_e is the equilibrium Cr (VI) concentration in liquid phase (mg L^{-1}), C_t is the Cr (VI) concentration in liquid phase at time t (mg L^{-1}), m is amount of chitosan (g), and V is the volume of solution (L).

2.3. Response surface methodology

The adsorption capacity of metal ions by chitosan is influenced by several factors, such as amounts of adsorbent and adsorbate, temperature, stirring rate, particle size, pH of solution, and DD [5,21]. Among these, the pH and the DD were the most important [5,14]. In order to verify the influence of these factors, and so, to optimize the adsorption process, response surface methodology was employed [28]. The levels and factors were selected by preliminary tests and literature [5,14,20,21] and are showed in Table 1. The Cr (VI) adsorption capacity (q) was represented as function of independent variables according to Eq. (4):

$$q = a + \sum_{i=1}^n b_i x_i + \sum_{i=1}^n b_{ii} x_i^2 + \sum_{i=1}^{n-1} \sum_{j=i+1}^n b_{ij} x_i x_j \quad (4)$$

where q is the predicted response, a the constant coefficient, b_i the linear coefficients, b_{ij} the interaction coefficients, b_{ii} the quadratic coefficients, x_i and x_j are the coded values of the variables.

The results were analyzed using Statistic version 7 (StatSoft Inc., USA) software. The second order model (Eq. (4)) was evaluated by Fischer's test, and the proportion of variance explained by the model was given by the multiple coefficient of determination, R^2 . The significance level was 95% ($p < 0.05$), and the nonsignificant factors were excluded [28].

2.4. Equilibrium isotherms

The experimental equilibrium data were evaluated at different temperatures (298–328 K) by Langmuir, Freundlich, Redlich–Peterson and Sips nonlinear isotherm models.

Table 1
Experimental design matrix and results for the Cr (VI) adsorption onto chitosan

Experiment	pH (coded value)	DD (%) (coded value)	q (mg g ⁻¹)*
1	3 (-1)	75 (-1)	12.1 ± 0.4
2	3 (-1)	85 (0)	14.5 ± 0.3
3	3 (-1)	95 (+1)	16.4 ± 0.1
4	4 (0)	75 (-1)	5.4 ± 0.1
5	4 (0)	85 (0)	5.9 ± 0.2
6	4 (0)	95 (+1)	7.3 ± 0.1
7	5 (+1)	75 (-1)	2.7 ± 0.2
8	5 (+1)	85 (0)	7.2 ± 0.2
9	5 (+1)	95 (+1)	7.9 ± 0.2

*Mean ± standard error ($n = 3$).

The Langmuir model assumes that the solid surface carries a limited number of sites that are characterized by equal adsorption energy, independent of the coverage degree, and thus, it indicates a monolayer adsorption [29]. The nonlinear Langmuir model is given by Eq. (5):

$$q_e = \frac{q_m k_L C_e}{1 + k_L C_e} \quad (5)$$

where C_e is the adsorbate equilibrium concentration (mg L⁻¹), q_e is the amount of solute adsorbed per mass unit of adsorbent (mg g⁻¹), q_m relates to the saturated adsorption capacity (mg g⁻¹) and k_L is related to the affinity of the adsorbate for the adsorbent (L mg⁻¹).

The nonlinear Freundlich model assumes that the adsorption surface is heterogeneous and can be represented by the Eq. (6) [30]:

$$q_e = k_F C_e^{1/n} \quad (6)$$

where k_F is the Freundlich constant ((mg g⁻¹) (mg L⁻¹)^{-1/n}) and $1/n$ is the heterogeneity factor.

The nonlinear Redlich–Peterson model is used to represent adsorption equilibrium over a wide concentration range and can be applied either in homogeneous or in heterogeneous systems due to its versatility [31].

$$q_e = \frac{k_R C_e}{1 + a_R C_e^\beta} \quad (7)$$

where k_R and a_R are the Redlich–Peterson constants (L g⁻¹) and (L mg⁻¹), respectively, and β is the heterogeneity coefficient (which varies between 0 and 1).

The nonlinear Sips model is a Langmuir and Freundlich isotherm combination. This model at low adsorbate concentrations reduces to Freundlich model and thus does not obey Henry's Law. At high concentrations, adsorbate predicts a monolayer adsorption characteristic of Langmuir isotherm [32]. The nonlinear Sips model is represented by Eq. (8):

$$q_e = \frac{q_{ms} (K_s C_e)^m}{(1 + (K_s C_e)^m)} \quad (8)$$

where q_{ms} (mg g⁻¹) is the maximum adsorption capacity of Sips, K_s (L mg⁻¹) the Sips constant and m the exponent of Sips model.

2.5. Kinetic models

The kinetic data were evaluated at different stirring rates (50–350 rpm) by nonlinear pseudo-first order, pseudo-second order and Elovich models.

The nonlinear kinetic models of pseudo-first order and pseudo-second order assume that adsorption is a pseudo-chemical reaction, and the adsorption rate can be determined, respectively, for equations of pseudo-first (Eq. (9)) [33] and pseudo-second order (Eq. (10)) [34]:

$$q_t = q_1(1 - \exp(-k_1 t)) \quad (9)$$

$$q_t = \frac{t}{(1/k_2 q_2^2) + (t/q_2)} \quad (10)$$

where k_1 and k_2 are the rate constants of pseudo-first-order model and pseudo-second order model, respectively, in (min^{-1}) and ($\text{g mg}^{-1} \text{min}^{-1}$), q_1 and q_2 are the theoretical values for the adsorption capacity (mg g^{-1}) and t is the time (min).

The Elovich kinetic model is described by Eq. (11) [35]:

$$q_t = \frac{1}{a} \ln(1 + abt) \quad (11)$$

where a is the initial sorption rate due to dq/dt with $q_t=0$ ($\text{mg g}^{-1} \text{min}^{-1}$) and b is the desorption constant of the Elovich model (g mg^{-1}).

The kinetic and isotherm parameters were estimated by nonlinear regression using Statistica 7.0 software (Statsoft, USA). The objective function was Quasi-Newton. The fit quality was evaluated by coefficient of determination (R^2) and average relative error (ARE) Eq. (12):

$$\text{ARE} = \frac{100}{n} \sum \left| \frac{q_{t,\text{exp}} - q_{t,\text{pre}}}{q_{t,\text{exp}}} \right| \quad (12)$$

where $q_{t,\text{exp}}$ and $q_{t,\text{pre}}$ are the experimental and theoretical adsorption capacity values.

2.6. Thermodynamic analysis

The adsorption characteristics of a material can be expressed in terms of thermodynamic parameters, such as, ΔG^0 (kJ mol^{-1}) (Gibbs free energy change), which can be calculated by Eq. (13) [36]:

$$\Delta G^0 = -RT \ln(55.5 K_D) \quad (13)$$

where K_D is the thermodynamic equilibrium constant (L mol^{-1}), and 55.5 is the number of moles of water per liter of solution (mol L^{-1}), T is the temperature (K) and R is the universal gas constant ($8.314 \text{ J mol}^{-1} \text{ K}^{-1}$).

The K_D values were estimated from the parameters of the best fit isotherm model [36–38].

The Gibbs free energy change is the difference between the adsorption enthalpy change (ΔH^0) (kJ mol^{-1}) and adsorption entropy change (ΔS^0) ($\text{kJ mol}^{-1} \text{K}^{-1}$) multiplied by the temperature [36]. This manner, by applying this concept to Eq. (13), the values of ΔH^0 and ΔS^0 can be estimated using Van't Hoff's plot, according to Eq. (14) [36,37]:

$$\ln(55.5 K_D) = \frac{\Delta S^0}{R} - \frac{\Delta H^0}{RT} \quad (14)$$

2.7. Interactions Cr (VI)—Chitosan

In order to verify the possible interactions between Cr (VI) and chitosan, samples were analyzed before and after adsorption process (in the best condition) using FT-IR analysis (Prestige, 21210045, Japan) [26] and EDS (Dispersive energy X-ray spectroscopy) (Jeol, JSM-5800, Japan) [39].

3. Results and discussion

3.1. Chitosan characterization

The chitosan DD obtained at different reaction times (40, 90 and 240 min) were $75.0\% \pm 1.3$, $85.0\% \pm 1.5$ and $95.0\% \pm 0.9$, and the viscosity average molecular weights were 212 ± 4 , 150 ± 3 and $120 \pm 4 \text{ kDa}$, respectively. These values are in accordance with the deacetylation kinetic found by Moura et al. [23]. In order to identify changes in functional groups, chitosan samples with different DD were analyzed by FT-IR. Fig. 1 shows the FT-IR spectrum of chitosan with different DD.

In Fig. 1, the chitosan characteristic stretches of N–H and O–H were observed at $3,350$ and $3,150 \text{ cm}^{-1}$. The C–N stretching of amides was identified at $1,550 \text{ cm}^{-1}$. The angular deformations of C–O–H and H–C–H appeared at $1,450 \text{ cm}^{-1}$. At $1,075 \text{ cm}^{-1}$, the C–N stretching related to the amino groups was identified. The most relevant changes in Fig. 1 were identified between $1,600$ and $1,700 \text{ cm}^{-1}$.

In the Fig. 1(a), there is an overlap of C=O stretching bond of amide on the angular deformation of N–H. However, a decrease in the C=O intensity and the separation of bands can be observed in Fig. 1(b) and 1(c). These changes confirm the DD increase during the reaction. Moura et al. [23] demonstrated that the DD is dependent of the reaction time.

Fig. 2 shows the XRD of chitin (Fig. 2(a)) and chitosan with different DD (Fig. 2(b–d)). Based on the

intense and narrow peaks presented in XRD, it was found that all biopolymers have predominantly crystalline structure. However, during the deacetylation reaction, changes occurred in the crystalline planes, due to changes in the interactions between the biopolymers chains. This behavior can be observed due to appearance of new peaks, mainly between

chitin (Fig. 2(a)) and chitosan DD75% (Fig. 2(b)), and between chitosan DD75 and DD85% (Fig. 2(c)).

3.2. RSM results

Table 1 shows the experimental design matrix with the results for the Cr (VI) adsorption by chitosan with different DD.

The analysis of variance of the results presented in Table 1 showed that the pH and DD were significant ($p < 0.05$) in relation to the Cr (VI) adsorption capacity. The statistical polynomial quadratic model that represents the dependence of Cr (VI) adsorption capacity in relation to the pH (x_1) and DD (x_2) is given by Eq. (15):

$$q = 6.6 + 3.9x_1^2 - 0.6x_2^2 - 4.2x_1 + 1.9x_2 \quad (15)$$

In order to verify the prediction and significance of the statistical model (Eq. (15)), analysis of variance and Fischer's F -test were employed. The high values of coefficient of determination ($R^2 = 0.97$) showed that the model was significant. The calculated F value ($F_{CALC} = 93.6$) was about 30 times higher than standard F value ($F_{TAB} = 3.2$) showing that the model was

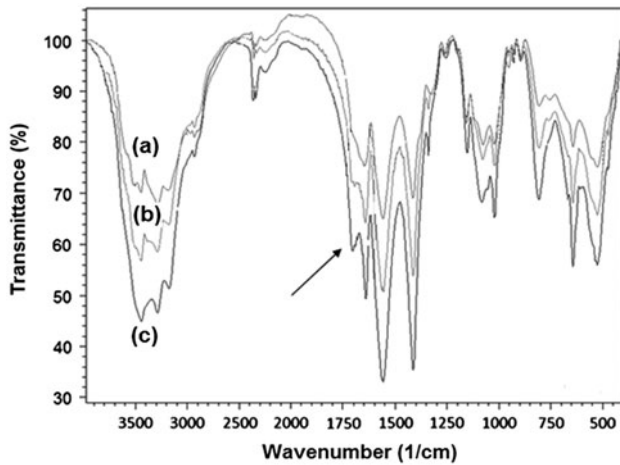


Fig. 1. FT-IR spectrum of chitosan with different DD.

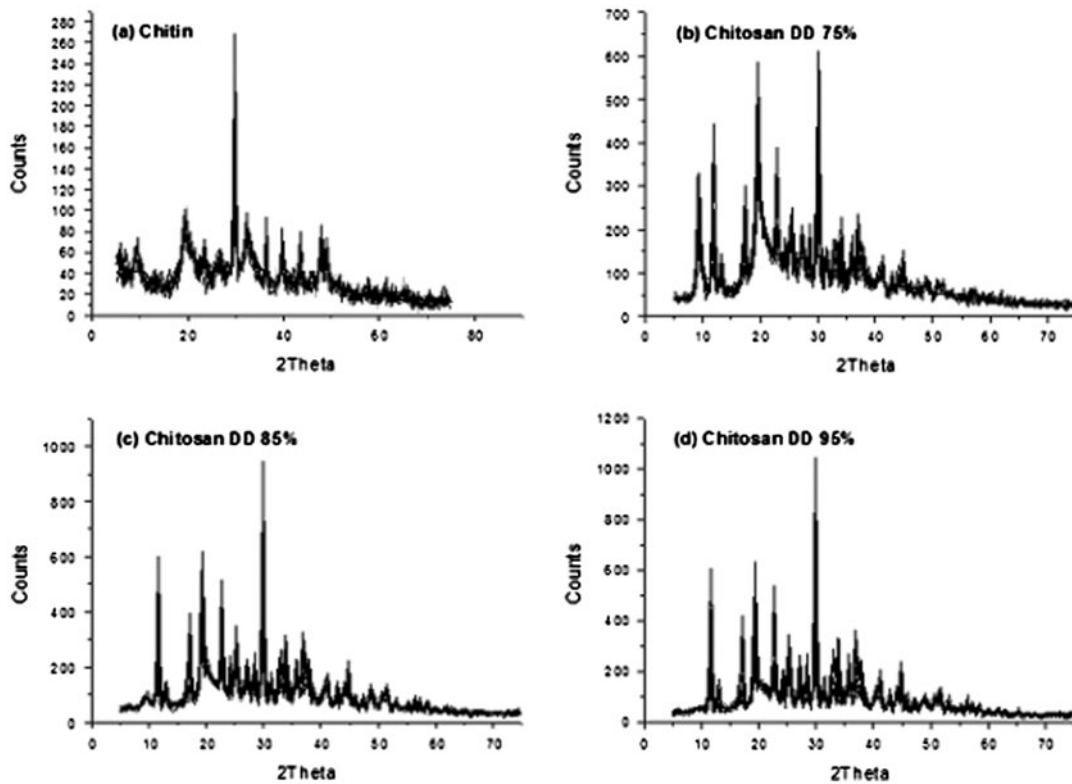


Fig. 2. XRD of chitin and chitosan with different DD.

predictive. Then, the statistical model was used to generate the response surface (Fig. 3), which represents the Cr (VI) adsorption capacity as a function of independent variables.

Fig. 3 shows that the Cr (VI) adsorption capacity increased with the pH decrease and DD increase. This behavior can be explained by the adsorption mechanism of chromium by chitosan in acidic conditions. Under acid conditions, the hydrogen atoms (H^+) in solution tend to protonate chitosan amino groups ($-NH_2$) [5]. Coupled to this, different species of anionic Cr (VI) ($Cr_2O_7^{2-}$, $HCrO_4^-$, $Cr_3O_{10}^{2-}$, $Cr_4O_{13}^{2-}$) coexist [40]. This manner, the process occurs through electrostatic interactions between anionic Cr (VI) and chitosan-protonated amino groups [5]. In this work, the pH decrease and the DD increase led to the protonation of more chitosan amino groups, increasing the adsorption sites, and consequently, the Cr (VI) adsorption capacity was increased. Similar results in relation to the pH effect were found by Aydin and Aksoy [20] in the adsorption of Cr (VI) onto chitosan. According to Crini and Badot [21] at pH values below 3, a large excess of competitor ions limit the adsorption efficiency. Piccin et al. [41] reported that the DD increase contributed to increase in the adsorption capacity of the FD & C red No. 40 dye onto chitosan.

In the considered range, the more appropriate conditions for the Cr (VI) adsorption onto chitosan obtained by the response surface (Fig. 3) were: pH 3 and DD of 95%. Under these conditions, the Cr (VI) adsorption capacity was 16.0 mg g^{-1} .

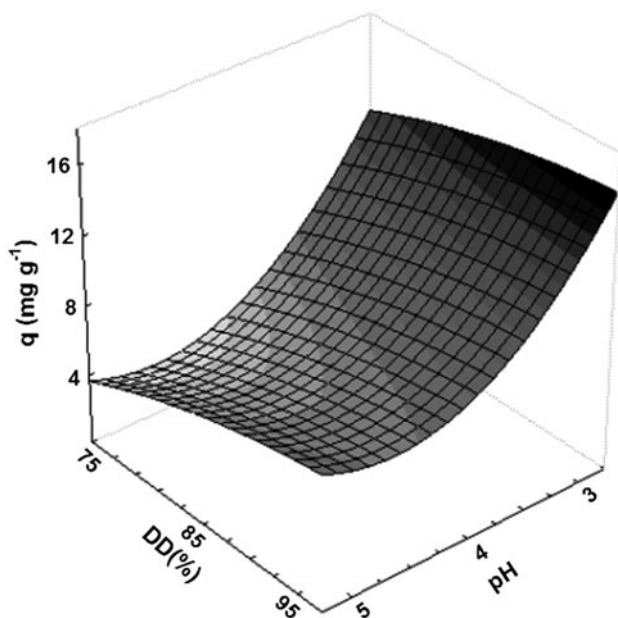


Fig. 3. Cr (VI) adsorption capacity as a function of pH and DD.

3.3. Isotherms and thermodynamics

The equilibrium adsorption isotherms were obtained from 298 to 328 K, using chitosan with 95% of DD at pH 3. Fig. 4 shows the equilibrium experimental data of Cr (VI) adsorption onto chitosan in all studied temperatures.

In Fig. 4 the isotherms were characterized by an initial increase in the adsorption capacity (indicating the great affinity between chitosan and Cr (VI) and a large number of accessible sites), tending a convex shape, which is associated with monolayer adsorption [10]. In this figure, the temperature increase caused a decrease in adsorption capacity was observed. This can have occurred due to the temperature increase to cause an increase in the Cr (VI) solubility [5], so the interaction forces between Cr (VI) and the solvent become stronger than those between Cr (VI) and chitosan. Similar behavior was reported by Aydin and Aksoy [20].

In order to establish the most appropriate correlation to the equilibrium curves and estimate the isotherm parameters, four models (Langmuir, Freundlich, Redlich–Peterson and Sips) were fitted to the experimental data. Table 2 shows the isotherm parameters of Cr (VI) adsorption chitosan in all studied temperatures.

Table 2 shows that the Sips model was the more appropriate to fit the equilibrium experimental data in all studied conditions ($R^2 > 0.99$ and $ARE < 2.5\%$). The maximum adsorption capacity (q_{ms}) increased with the temperature decrease, reaching a maximum value of 97.4 mg g^{-1} at 298 K. The literature shows values in the range from 2.8 to 110 mg g^{-1} for Cr (VI) adsorption onto various adsorbents [1,5,20,42,43]. This shows that chitosan used in this study presented a good adsorption capacity.

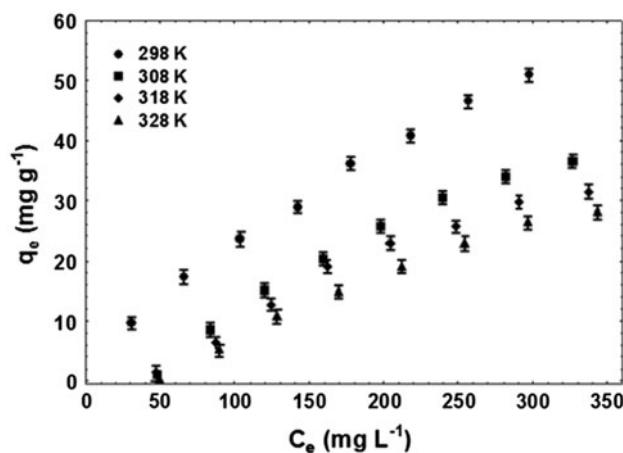


Fig. 4. Equilibrium experimental data of Cr (VI) adsorption onto chitosan in all studied temperatures.

Table 2
Isotherm parameters for Cr (VI) adsorption onto chitosan

Model	298 K	308 K	318 K	328 K
<i>Langmuir</i>				
q_m (mg g ⁻¹)	128.0	236.4	142.1	220.8
$k_L \times 10^3$ (L mg ⁻¹)	2.2	0.5	0.8	0.4
R^2	0.997	0.972	0.959	0.965
ARE (%)	3.86	6.76	11.85	24.43
<i>Freundlich</i>				
k_F (mg g ⁻¹) (L mg ⁻¹) ^{-1/n}	0.705	0.117	0.103	0.063
n	1.36	0.99	1.01	0.90
R^2	0.999	0.973	0.967	0.975
ARE (%)	1.33	6.48	9.72	7.78
<i>Redlich–Peterson</i>				
k_R (L mg ⁻¹)	0.383	0.356	0.106	0.088
a_R (L mg ⁻¹) ^{β}	0.0450	1.9980	0.0003	0.0331
B	0.5800	0.0001	0.9071	0.0002
R^2	0.998	0.972	0.968	0.971
ARE (%)	1.61	6.46	9.81	8.60
<i>Sips</i>				
q_{mS} (mg g ⁻¹)	97.4	45.1	36.0	35.9
K_L (L mg ⁻¹)	0.002	0.006	0.006	0.005
m	0.82	2.18	2.45	2.29
R^2	0.998	0.996	0.997	0.996
ARE (%)	1.41	2.38	2.24	2.11

The thermodynamic adsorption behavior of Cr (VI) by chitosan was measured by changes of enthalpy, entropy and Gibbs free energy. These values are shown in Table 3. The K_D values were estimated from the Sips parameters [36–38].

The negative ΔG^0 values (Table 3) indicated that the Cr (VI) adsorption by chitosan was a spontaneous and favorable process. The negative ΔH^0 values (Table 3) show that the adsorption process was exothermic. The negative ΔS^0 values (Table 3) indicated that the disorder in the solid–liquid interface decreased during the adsorption process. Comparing ΔH^0 and ΔS^0 values, it can be seen that the enthalpy is most relevant than entropy to obtain the negative ΔG^0 values, showing that Cr (VI) adsorption by chitosan was predominantly an enthalpy controlled process. Similar thermodynamic behavior was found by Piccin et al. [44] in the adsorption of FD and C red No. 40 by chitosan, and these authors showed that the adsorption was exothermic, spontaneous favorable.

3.4. Kinetic analysis:

The kinetic analysis was carried out using chitosan with 95% of DD at pH 3 and 298 K. The stirring rate

Table 3
Thermodynamic parameters for the Cr (VI) adsorption onto chitosan

Temperature (K)	ΔG (kJ mol ⁻¹)*	ΔH (kJ mol ⁻¹)*	ΔS (kJ mol ⁻¹ K ⁻¹)* $\times 10^3$
298	-4.87 ± 0.01	-6.57 ± 0.10	-5.77 ± 0.01
308	-4.80 ± 0.01		
318	-4.75 ± 0.02		
328	-4.68 ± 0.01		

*Mean ± standard error ($n = 3$).

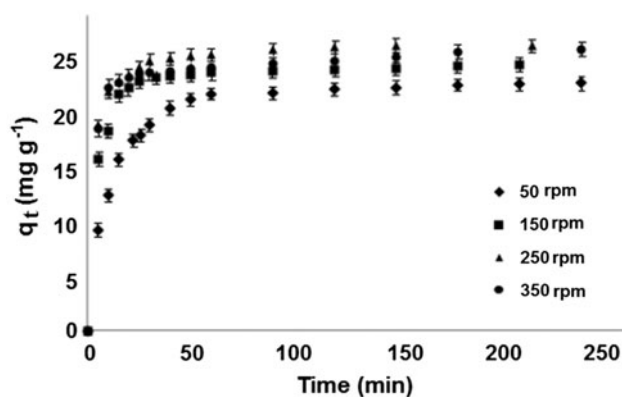


Fig. 5. Adsorption capacity of Cr (VI) by chitosan in different stirring rates.

effect was studied under stirring rates ranging from 50 to 350 rpm, and the results are showed in Fig. 5.

From the kinetic curves (Fig. 5), it was observed that adsorption was initially fast reaching about 80% of saturation at 50 min. After the adsorption rate decreased considerably, being that the equilibrium was attained at 48 h. Aydin and Aksoy [20] found similar results. The stirring rate increase from 50 to 150 rpm caused an increase in the adsorption rate. However, a new increase until 350 rpm presented a little effect (Fig. 5). This behavior can be explained because an increase in the degree of agitation increased the mobility of the system. In addition, agitation increase by increase of stirrer speed lowers the external mass transfer effect [45].

To elucidate the adsorption kinetics, the reaction kinetic models Eqs. (9–11) were fitted with the experimental data. These results are showed in Table 4. It was found in Table 4 that pseudo-second-order model was the more adequate to represent the experimental kinetic data ($R^2 > 0.99$ and $ARE < 2.00$). Furthermore, q_2 values (Table 4) are in agree with the equilibrium experimental adsorption capacity ($q_e \text{ exp} = 26.1 \text{ mg g}^{-1}$). The k_2 values (Table 4) increased as a function of the stirring rate increase, showing that adsorption occurred faster at higher stirring rates.

Table 4
Kinetic parameters for Cr (VI) adsorption onto chitosan

Kinetic model	Stirring rate (rpm)			
	50	150	250	350
<i>Pseudo-first order</i>				
q_1 (mg g ⁻¹)	22.3	23.9	25.5	24.8
k_1 (min ⁻¹)	0.077	0.177	0.231	0.254
R^2	0.981	0.982	0.975	0.976
ARE (%)	4.16	2.91	3.77	3.51
<i>Pseudo-second order</i>				
q_2 (mg g ⁻¹)	23.8	24.9	26.5	25.7
k_2 (g mg ⁻¹ min ⁻¹)	0.005	0.014	0.017	0.020
R^2	0.999	0.999	0.999	0.999
ARE (%)	1.48	1.41	0.81	1.74
<i>Elovich</i>				
a (g mg ⁻¹)	0.34	0.59	0.69	0.74
b (mg g ⁻¹ min ⁻¹)	41.8	22786.8	657661.0	1464300.0
R^2	0.859	0.737	0.842	0.873
ARE (%)	7.36	4.82	7.69	5.02

3.5. Interactions Cr (VI)–chitosan

The chitosan DD95% infrared spectrum (Fig. 6(a)) before adsorption shows the same bands in relation to

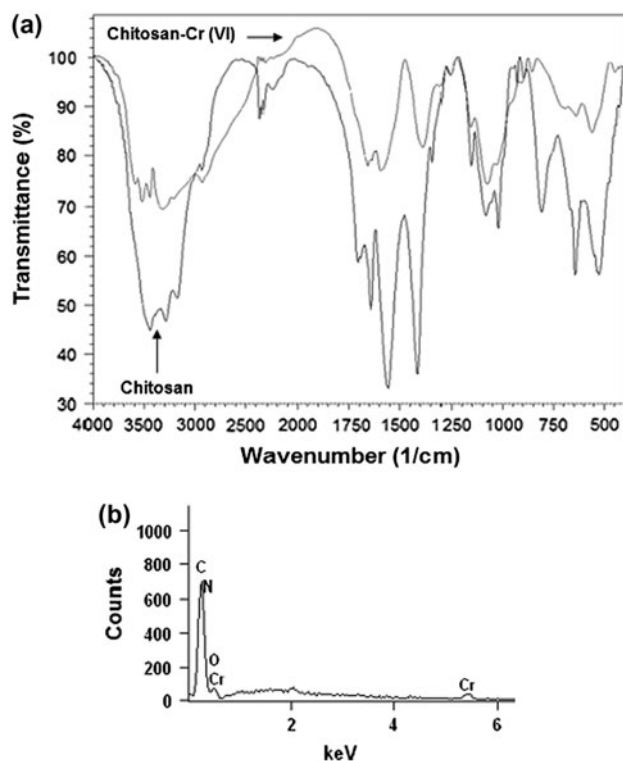


Fig. 6. (a) Chitosan DD 95% infrared spectrum before and after adsorption and (b) EDS spectrum of chitosan after the adsorption process.

the spectrum of Fig. 1(c). On the other hand, after Cr (VI) adsorption, changes in functional groups were observed. The changes occurred mainly in N–H stretching (3,350 cm⁻¹), angular deformation of N–H (1,617 cm⁻¹) and angular deformation of H–N–H (680 cm⁻¹). This shows the preferably of Cr (VI) for the chitosan-protonated amino group. The presence of Cr in the EDS spectrum of chitosan after adsorption (Fig. 6(b)) confirms the interaction of chitosan–Cr (VI).

4. Conclusions

This work studied the use of chitosan with different DD to remove Cr (VI) from aqueous solutions by adsorption. Chitosan samples obtained from shrimp wastes showed DD between 75 and 95% and molecular weight in the range from 120 to 212 kDa. The DD increase caused changes in crystallinity.

The more appropriate conditions for Cr (VI) adsorption by chitosan were at pH 3 and DD of 95%. The Sips model was the most adequate to represent the equilibrium adsorption isotherms ($R^2 > 0.99$ and $ARE < 2.5\%$). The maximum adsorption capacity was 97.4 mg g⁻¹ obtained at 298 K. The negative values of ΔG^0 , ΔH^0 and ΔS^0 showed that the Cr (VI) adsorption by chitosan was a spontaneous favorable and exothermic process. The pseudo-second-order model presented adequate fit with the experimental kinetic data ($R^2 > 0.99$ and $ARE < 2.00$). FT-IR and EDS analysis suggested that interactions between Cr (VI) and chitosan-protonated amino groups occurred.

Acknowledgment

The authors would like to thank CAPES (Brazilian Agency for Improvement of Graduate Personnel) and CNPq (National Council of Science and Technological Development) for the financial support.

References

- [1] A.B. Albadarin, C. Mangwandi, A.H. Al-Muhtaseb, G.M. Walker, S.J. Allen, M.M. Ahmad, Kinetic and thermodynamics of chromium ions adsorption onto low-cost dolomite adsorbent, *Chem. Eng. J.* 179 (2012) 193–202.
- [2] W.S. Wan Ngah, A. Kamari, S. Fatinathan, P.W. Ng, Adsorption of chromium from aqueous solution using chitosan beads, *Adsorption* 12 (2006) 249–257.
- [3] I. Ali, M. Asim, T.A. Khan, Low cost adsorbents for the removal of organic pollutants from wastewater, *J. Environ. Manage.* 113 (2012) 170–183.
- [4] R.B. Garcia-Reyes, J.R. Rangel-Mendez, Adsorption kinetics of chromium (III) ions on agro-waste materials, *Bioresour. Technol.* 101 (2010) 8099–8108.
- [5] E. Guibal, Interactions of metal ions with chitosan-based sorbents: A review, *Sep. Purif. Technol.* 38 (2004) 43–74.
- [6] H. Wang, C. Li, C. Bao, L. Liu, X. Liu, Adsorption and determination of Pd(II) and Pt(IV) onto 30-Nitro-4-amino azobenzene modified chitosan, *J. Chem. Eng. Data* 56 (2011) 4203–4207.
- [7] E. Nathaniel, A. Kurniawan, F.E. Soetredjo, S. Ismadji, Organo-bentonite for the adsorption of Pb(II) from aqueous solution: Temperature dependent parameters of several adsorption equations, *Desal. Wat. Treat.* 36 (2011) 280–288.
- [8] X.S. Wang, F. Liu, H.J. Lu, P. Zhang, H.Y. Zhou, Adsorption kinetics of Cd (II) from aqueous solution by magnetite, *Desal. Wat. Treat.* 36 (2011) 203–209.
- [9] A.K. Hegazy, N.T. Abdel-Ghanib, G.A. El-Chaghabyc, Factorial design for optimizing the removal of aluminium from aqueous solutions by adsorption on *Typha domingensis* phytomass, *Desal. Wat. Treat.* 36 (2011) 392–399.
- [10] G. Blázquez, M. Calero, F. Hernáinz, G. Tenorio, M.A. Martín-Lara, Equilibrium biosorption of lead(II) from aqueous solutions by solid waste from olive-oil production, *Chem. Eng. J.* 160 (2010) 615–622.
- [11] L. Pelit, F.N. Ertaş, A.E. Eroğlu, T. Shahwan, H. Tural, Biosorption of Cu(II) and Pb(II) ions from aqueous solution by natural spider silk, *Bioresour. Technol.* 102 (2011) 8807–8813.
- [12] M.A. Javed, H.N. Bhatti, M.A. Hanif, R. Nadeem, Kinetic and equilibrium modeling of Pb(II) and CO(II) sorption onto rose waste biomass, *Sep. Sci. Technol.* 42 (2007) 3641–3656.
- [13] N.S. Barot, H.K. Bagla, Eco-friendly waste water treatment by cow dung powder (Adsorption studies of Cr(III), Cr(VI) and Cd(II) using tracer technique), *Desal. Wat. Treat.* 38 (2012) 104–113.
- [14] W.S. Wan Ngah, L.C. Teong, M.A.K.M. Hanafiah, Adsorption of dyes and heavy metal ions by chitosan composites: A review, *Carbohydr. Polym.* 83 (2011) 1446–1456.
- [15] L. Zhou, J. Jin, Z. Liu, X. Liang, C. Shang, Adsorption of acid dyes from aqueous solutions by the ethylenediamine-modified magnetic chitosan nanoparticles, *J. Hazard. Mater.* 185 (2011) 1045–1052.
- [16] P.O. Osifo, A. Webster, H. Van der Merwe, H.W.J.P. Neomagus, M.A. Van der Gun, D.M. Grant, The influence of the degree of cross-linking on the adsorption properties of chitosan beads, *Bioresour. Technol.* 99 (2008) 7377–7382.
- [17] C.M. Futralan, C.C. Kan, M.L. Dalida, K.J. Hsien, C. Pascua, M. Wan, Comparative and competitive adsorption of copper, lead, and nickel using chitosan immobilized on bentonite, *Carbohydr. Polym.* 83 (2010) 528–536.
- [18] H.H. Santos, C.A. Demarchi, C.A. Rodrigues, M. Greneche, N. Nedelko, A.S. Lawska-Waniewska, Adsorption of As(III) on chitosan-Fe-crosslinked complex (Ch-Fe), *Chemosphere* 82 (2011) 278–283.
- [19] M. Benavente, L. Moreno, J. Martinez, Sorption of heavy metals from gold mining wastewater using chitosan, *J. Taiwan Inst. Chem. Eng.* 42 (2011) 976–988.
- [20] Y.A. Aydin, N.D. Aksoy, Adsorption of chromium on chitosan: Optimization, kinetics and thermodynamics, *Chem. Eng. J.* 151 (2009) 188–194.
- [21] G. Crini, P.M. Badot, Application of chitosan, a natural aminopolysaccharide, for dye removal from aqueous solutions by adsorption processes using batch studies: A review of recent literature, *Prog. Polym. Sci.* 33 (2008) 399–447.
- [22] R.F. Weska, J.M. Moura, L.M. Batista, J. Rizzi, L.A.A. Pinto, Optimization of deacetylation in the production of chitosan from shrimp wastes: Use of response surface methodology, *J. Food Eng.* 80 (2007) 749–753.
- [23] C.M. Moura, J.M. Moura, N.M. Soares, L.A.A. Pinto, Evaluation of molar weight and deacetylation degree of chitosan during chitin deacetylation reaction: Used to produce biofilm, *Chem. Eng. Proces.* 50 (2011) 351–355.
- [24] G.L. Dotto, V.C. Souza, L.A.A. Pinto, Drying of chitosan in a spouted bed: The influences of temperature and equipment geometry in powder quality, *LWT-Food Sci. Technol.* 44 (2011) 1786–1792.
- [25] X. Jiang, L. Chen, W.I. Zhong, A new linear potentiometric titration method for the determination of deacetylation degree of chitosan, *Carbohydr. Polym.* 54 (2003) 457–463.
- [26] R.M. Silverstein, F.X. Webster, D.J. Kiemle, *Spectrometric identification of organic compounds*, Wiley, New York, NY, 2007.
- [27] J. Kumirska, M. Czerwicka, Z. Kaczyński, A. Bychowska, K. Brzozowski, J. Thöming, P. Stepnowski, Application of spectroscopic methods for structural analysis of chitin and chitosan, *Mar. Drugs* 8 (2010) 1567–1636.
- [28] R.H. Myers, D.C. Montgomery, *Response surface methodology: Process and product optimization using designed experiments*, Wiley, New York, NY, 2002.
- [29] I. Langmuir, The adsorption of gases on plane surfaces of glass, mica and platinum, *J. Amer. Chem. Soc.* 40 (1918) 1361–1403.
- [30] H. Freundlich, Over the adsorption in solution, *Z. Physic. Chem.* A57 (1906) 358–471.
- [31] O. Redlich, D.L. Peterson, A useful adsorption isotherm, *J. Chem. Phys.* 63 (1959) 1024–1027.
- [32] R. Sips, On the structure of a catalyst surface, *J. Chem. Phys.* 16 (1948) 490–495.
- [33] H. Qiu, L.L. Pan, Q.J. Zhang, W. Zhang, Q. Zhang, Critical review in adsorption kinetic models, *J. Zhejiang Univ. Sci. A* 10 (2009) 716–724.
- [34] Y.S. Ho, G. Mckay, Kinetic models for the sorption of dye from aqueous solution by wood, *Proc. Safety Environ. Protect.* 76 (1998) 183–191.
- [35] F.C. Wu, R.L. Tseng, R.S. Juang, Characteristics of Elovich equation used for the analysis of adsorption kinetics in dye chitosan systems, *Chem. Eng. J.* 150 (2009) 366–373.
- [36] S.K. Milonjić, A consideration of the correct calculation of thermodynamic parameters of adsorption, *J. Serb. Chem. Soc.* 72 (2007) 1363–1367.
- [37] Y. Liu, Is the free energy change of adsorption correctly calculated? *J. Chem. Eng. Data* 54 (2009) 1981–1985.
- [38] G.L. Dotto, E.C. Lima, L.A.A. Pinto, Biosorption of food dyes onto *Spirulina platensis* nanoparticles: Equilibrium isotherm and thermodynamic analysis, *Bioresour. Technol.* 103 (2012) 123–130.
- [39] D. Hritcu, D. Humelnicu, G. Dodi, M.I. Popa, Magnetic chitosan composite particles: Evaluation of thorium and uranyl ion adsorption from aqueous solutions, *Carbohydr. Polym.* 87 (2012) 1185–1191.

- [40] P. Yuan, D. Liu, M. Fan, D. Yang, R. Zhu, F. Ge, J. Zhu, H. He, Removal of hexavalent chromium [Cr(VI)] from aqueous solutions by the diatomite-supported/unsupported magnetite nanoparticles, *J. Hazard. Mater.* 173 (2010) 614–621.
- [41] J.S. Piccin, M.L.G. Vieira, J.O. Gonçalves, G.L. Dotto, L.A.A. Pinto, Adsorption of FD & C Red No. 40 by chitosan: Isotherms analysis, *J. Food Eng.* 95 (2009) 16–20.
- [42] H. Demiral, I. Demiral, F. Tumsek, B. Karabacakoglu, Adsorption of chromium (VI) from aqueous solution by activated carbon derived from olive bagasse and applicability of different adsorption models, *Chem. Eng. J.* 144 (2007) 188–196.
- [43] A.H. Sulaymon, B.A. Abid, J.A. Al-Najar, Removal of lead copper chromium and cobalt ions onto granular activated carbon in batch and fixed-bed adsorbers, *Chem. Eng. J.* 155 (2009) 647–653.
- [44] J.S. Piccin, G.L. Dotto, L.A.A. Pinto, Adsorption isotherms and thermochemical data of FD & C Red No. 40 binding by chitosan, *Braz. J. Chem. Eng.* 28 (2011) 295–304.
- [45] G.L. Dotto, L.A.A. Pinto, Adsorption of food dyes acid blue 9 and food yellow 3 onto chitosan: Stirring rate effect in kinetics and mechanism, *J. Hazard. Mater.* 187 (2011) 164–170.